Bacteriophage richness reduces bacterial niche overlap in experimental microcosms

Miguel G. Matias[1,2,3], Dominique Gravel[4,5], Marine Combe[6], Timothee Poisot[7], Claire Barbera[1], Manon Lounnas[8], Thierry Bouvier and Nicolas Mouquet[1]

Affiliations:

[1] Institut des Sciences de l'Evolution, UMR 5554, CNRS, Université Montpellier 2, CC 065, Place Eugène Bataillon, 34095 Montpellier Cedex 05, France.

[2] InBio/CIBIO, Universidade de Évora, Largo dos Colegiais, 7000 Évora, Portugal

[3] Imperial College London, Silwood Park Campus, Buckhurst Road, SL5 7PY Ascot, Berkshire, United Kingdom.

[4] Université du Québec à Rimouski, Département de biologie, chimie et géographie, 300 Allée des Ursulines, Québec, Canada. G5L 3A1.

[5] Quebec Center for Biodiversity Science, Quebec, Canada

[6] Instituto Cavanilles de Biodiversidad y Biología Evolutiva, Valencia, Spain

[7] Université de Montréal, Départment des sciences biologiques, 90 Avenue Vincent d'Indy, H2V2S9 Montréal QC, Canada.

[8] MIVEGEC, UMR IRD 224 CNRS 5290 UM, 911 Avenue Agropolis, BP 64501, 34394 Montpellier Cedex 5, France

[9] Laboratoire Ecologie des Systèmes Marins Côtiers ECOSYM, UMR 5119, CNRS, IRD, Ifremer, Université Montpellier 2, Montpellier, France

Keywords: bacteriophages, bacteria, ecosystem-functioning, microcosms, overyielding, niche overlap

Corresponding author: Miguel G. Matias: Imperial College London, Silwood Park Campus, Buckhurst Road, SL5 7PY Ascot, Berkshire, United Kingdom. Email address: m.matias@imperial.ac.uk

28 **ABSTRACT (175/ 200)**

29 Antagonistic interactions such as competition and predation shape the structure and
30 dynamics of ecological communities. Their combined effects can affect the species
31 richness within a particular trophic level. Despite theory linking the complementarity of
32 interactions across trophic levels and ecosystem functioning, there is a shortage of
33 empirical tests of such predictions. We present an experimental investigation of these
34 combined effects within a bacteria-phage interaction network. We measured the
35 biomass yield of combinations of bacterial strains under increasing levels of
36 bacteriophage richness. Our results show an increasing impact of phage on bacterial
37 population growth with increasing phage diversity. In contrast, no combination of
38 phages significantly changed the overall productivity of bacterial mixed cultures when
39 compared with expectations based on bacterial monocultures. Finally, we found that the
40 addition of phages decreases the realized niche overlap among pair of bacterial species
41 with the greatest reduction occurring when all phages were present. Our results show
42 that the productivity of this system is the results from the combined effects of
43 exploitative (shared resources between bacteria) and apparent (shared phages between
44 bacteria) competition.

45

INTRODUCTION

Despite widespread evidence of the importance of predator-prey interactions in natural communities (Andrewartha & Birch 1954; Holt 1977), exploitative competition is often considered the key factor behind both species diversity and the biodiversity-ecosystem functioning relationship (BEF). However, a more comprehensive view of species interactions is realized when competition for resource and predation are considered symmetrically. While having been recognized for a long time (e.g. MacArthur 1972; Holt 1984; Grover & Holt 1998) this generalized view of community organization has been formalized only recently by Chesson and Kuang (2008). They have provided a generalized framework where competition and predation act similarly to maintain species richness within a trophic level: coexistence is then possible when intraspecific competition exceeds interspecific competition or when intraspecific density feedback through predators is stronger than interspecific density feedback through predators.

This unified model allows addressing conjointly the role of complex interactions in the building of ecological communities and on the emerging properties at the ecosystem levels. For instance Poisot et al. (2013) used this formalism to study how trophic complementarity drives the BEF relationship in food webs. Resource complementarity is the differential use of resources by two (or more) species. In a mirroring way, predation complementarity is the differential effect of predators on two (or more) species. From this, it is predicted that ecosystem functioning declines when two species interact indirectly via shared predators because of enhanced top-down control (Poisot et al. 2013). This hypothesis is yet untested empirically, and we are not aware of any manipulative experiments that have measured the impact of species trophic complementarity on ecosystem functioning.

Here we present an experimental study that investigated the contribution of trophic complementarity in bacterial microcosms in the presence of bacteriophages. We predict that realized niche overlap (i.e. how much niche space is shared) among pairs of species should decrease in presence of enemies. We compare the biomass yield of bacteria competing for a heterogeneous food source in presence and absence of a mixture of phage. We find that, despite decreasing niche overlap, increasing the diversity of the bacteriophages still decrease the biomass yield of bacteria through strong top-down control. The most diverse mixtures of bacteriophage cause the greatest reduction of niche overlap among bacteria, demonstrating that bacteria species compete not only for their resource, but also indirectly via shared enemies.

MATERIAL AND METHODS

Sample collection and processing

We collected soil samples from farmlands in the region of Montpellier (France) between February and March 2012. For each location, sample areas were at least 1 m apart from each other. We chose untouched fine soils, sediments and water since they have been shown to yield greater abundances of phages than coarse soils (Goyal & Gerba 1979). Dry soils were avoided because there will be fewer particles. In each sample area, we cleared the top layer of the soil and dig a small hole about 10 cm deep. We collected ~ 5 g of dry weight of each sample with a sterile spatula into a 15 mL Falcon centrifuge tube and filled with M9 minimal salts solution ($0.1 gl^{-1}$ NH_4Cl, $6 gl^{-1}$ Na_2HPO_4, 3gl−1 KH_2PO_4, $0.5 gl^{-1}$ NaCl) buffer till 10 ml (Gómez & Buckling 2011). Each sample was mixed 1 min by vortexing with glass beads and then incubated for 24 h at 28°C. After 24 h, samples were vortexed again for 1 min and placed on ice for 20-

30 min to stop the metabolic activity of bacteria and phages. Samples were sonicated using an Ultrasonic Water bath (25 W; 38 Khz) for 3 periods of 1 min with alternatives resting periods of 1 min on ice. After this step, samples were centrifuged at 600 g for 30 minutes to remove all particulate matter.

Isolating bacterial strains

The supernatant of each sample (50 µl) were plated on two different medium, (i) the non-specific media KB medium (glycerol 10 $\mu l.l^{-1}$ + 20 $g.l^{-1}$ protease peptone H_3 + 1.5 $g.l^{-1}$ K_2HPO_4 + 1.5 $g.l^{-1}$ $MgSO_4$; autoclaved 20 min at 121°C) with agar and (ii) the *Pseudomonas* specific Gould S1 medium (sucrose, glycerol, casamino acids, $NaHCO_3$, $MgSO_4$ $7H_2O$, K_2HPO_4 $3H_2O$, N lauroyl sarcosine sodium, trimethoprim), and incubated for 24 h at 28°C. Single bacterial genotypes (e.g. individual colonies) were isolated from each petri-dish and amplified for 48h at 28°C in Falcon tubes filled with 5 ml of KB media. In parallel, the laboratory strain *Pseudomonas fluorescens* SBW25 was amplified in KB media, under the same conditions. Bacteria isolated (approx. 100 strains) were frozen with 80% Glycerol (40/60%, v/v) and stored at -80°C.

Isolating phage genotypes

Phages were isolated using locally sampled bacteria as hosts so that the each phage isolate was known to infect, and kill through lysis, at least one of the isolated bacterial. For the extraction of phages, chloroform (10% v:v) was added in 2 ml Eppendorf tubes with the remainder supernatant and the mix was centrifuged at 13000 rpm for 8 minutes. The resulting supernatant was filtrated with a 0.22 µm filters (Millipore filter) to remove any remaining bacteria. Two hundred microliters of each supernatant were amplified in 24 well-microplates, with 200 µl of each bacterial genotypes isolated from the same site and 1.6 ml of KB media, for 24 h at 28°C under alternative agitation (1

min at 120 rpm every 30 min). This procedure allowed to infect bacteria from a site with their respective phage and, thus to optimize the efficacy of phage amplification. Additionally, 200 µl of each phage supernatant were amplified with 200 µl of *Pseudomonas fluorescens SBW25* in KB, under the same culture conditions. For each mixture phage/bacteria, chloroform (10%, v:v) was added in 2 ml Eppendorf tubes to kill most of bacteria and tubes were centrifuged at 13000 rpm for 8 min. Bacterial lawns were poured in petri-dishes by adding 3% of fresh bacterial overnight in KB soft-agar. Three drops of 10 µl of phage dilutions (10^{-1} to 10^{-8}) were deposited on top of the bacterial lawns. After 12 h at room temperature, single plaques were picked from bacterial lawns and re-amplified in 200 µl of their specific bacterial host (host from which they were isolated) and 1.8 ml of KB, for 24 h at 28°C under alternative agitation (1 min at 120 rpm every 30 min). Isolated phage genotypes (approx. 120 genotypes) were frozen with bacteria at -80°C by adding 80% Glycerol (40/60% v/v).

Bacterial OTUs

We used the National Center for Biotechnology Information Basic Local Alignment Search Tool (BLAST; http://blast.ncbi.nlm.nih.gov/Blast.cgi) to characterize the bacterial OTUs. We screened all available microbial genomes within the NCBI database and selected the top 10 bacterial strains sharing 100% coverage and homology with each of the strains in our study. Preliminary analysis showed that isolated strains belong mainly to genus *Pseudomonas*, *Serratia*, *Enterobacter* or *Aeromonas* (see electronic supplementary material Table S1).

Interaction matrices

We built an infection matrix of all pairwise combinations between 17 bacterial strains and 48 phage strains. We used fresh bacterial overnight amplifications of each bacterial

strain (i.e. 6 ml of KB; 48 h at 28°C; under 200 rpm constant agitation). We centrifuged each culture for 5 min at 3500 rpm; removed the supernatant; re-suspend the pellet in 8 ml of M9 minimal salts solution and vortexed all tubes. This procedure removed any remaining KB from the amplification. We then transferred 200 µl of each bacterial strain to 96-well microplates and estimated bacterial cell densities by measuring optical density (OD) on a FLUOStar Optima Spectrophotometer (BMG LABTECH) at 650 nm – all measures were corrected for the optical density of the medium without bacteria. We proceeded to adjust bacterial densities to the mean cell density that was calculated by averaging OD values for each bacterial strain. The adjustment was done by diluting or concentrating bacterial cultures to match the target cell density, thus ensuring that all bacterial strains had similar initial cell densities.

The infection trial consisted of mixing 20 µl of phages and 20 µl of bacteria and 160 µl KB into a 96-well microplate. The same procedure was repeated for all pairwise combinations, which were randomly assigned to 96-well microplates. Relative cell densities were estimated immediately after the addition of phages using OD. All plates were then stored for 24 h at 28°C, under alternative agitation (1 min at 120 rpm, every 30 min). After 24 h, the strength for each interaction was estimated as the impact of the phage on the Malthusian fitness of the bacterial monoculture (Poisot et al. 2011):

$$Pij = \frac{ln\left(N_{ij24}/N_{ij,0}\right)}{ln\left(N_{ij,24}/N_{ij,0}\right)}$$

where N is the value of optical density (estimation of bacterial cell density size at time 0 and 24 h), and i and j are, respectively, bacteria strain and phage isolate.

Experimental design

Based on the results of the interactions matrices, we selected three phage isolates that showed consistent effects on bacterial strains from different sampling sites. We established individual 200 µl microcosms containing either monocultures or two-bacterial strain mixtures) and phages isolates (i.e. monocultures or three-phage mixtures). All microcosms were implemented in 96-well microplates previously filled with 160 µl KB medium. Mixed bacterial inoculums consisted of 10 µl of each bacterial strain in the mixtures; monocultures consisted of 20 µl of the same bacterial strain. All microplates were incubated for 2 h at 28°C without agitation to kickstart bacterial growth. After the established 2-hour period, we implemented five phage treatments with the addition of 20 µl of each phage isolate to each of the plates containing the bacterial cultures. We added phages to bacterial mixture in 5 different treatments: phage monocultures (P1, P2 or P3) by adding 20 µl of each phage isolate; phage mixtures (PMIX) by adding 20 µl of equal parts of P1, P2 and P3; control treatment by adding 20 µl of M9 minimal salts solution without phage. Bacterial densities were estimated immediately after the addition of phage by measuring optical density (OD) at 650 nm – all measures were corrected for the optical density of the medium without bacteria. OD provides an indirect measure of cell density and has been widely used to estimate relative changes in bacterial growth in experimental microcosms (Gravel et al. 2011; Livingston et al. 2012; Matias et al. 2013). All plates were then stored for 24 h at 28°C, under alternative agitation (1 min at 120 rpm, every 30 min). Optical density was measured again after 24 h. In the same way as explained above, the strength for each interaction was estimated as the impact of the phage on the Malthusian fitness of the bacterial monoculture.

Data analysis

We used three different response variables to investigate the effects of phages on bacterial mixtures: yield, overyielding and niche overlap. Yield (Y) is an estimate of bacterial population growth (or production) based on optical density 24 h after initial inoculation. In monocultures, yield is a measure of the growth of a single bacterial strain, while in mixtures it indicates the overall production of the community. Based on these estimates, we estimated overyielding (OV) of each pair of bacterial isolates using following formula:

$$OV_{ab} = \frac{Y_{ab}}{\max(Y_a, Y_b)}$$

where Y_{ab} is the yield of a mixture of bacterial strains *a* and *b*; Y_a and Y_b is the yield in monoculture of each of bacterial strains in the mixture. The average yield in monocultures is used as reference bacterial growth.

Finally, we derived niche overlap using the niche theory of Chesson and Kuang (Chesson & Kuang 2008) Calculations take in account yield in the mixtures and in monocultures under the presence or absence of phage (see electronic supplementary material, S2). The algebraic solution essentially reports a measure of the reduction of the density in mixtures caused by interactions relative to the carrying capacity.

RESULTS AND DISCUSSION

Our results showed a clear impact of phages on bacterial yield ($F_{4, 2715} = 240.5$; $P < 0.001$; Fig. 2a, b), with each phage separately having a significant effect on yield when compared to the cultures without phages. As predicted by the phage infection trials, each phage had a different level infection across the pool of bacterial hosts (P1 < P2 < P3; see multiple comparisons at $P < 0.05$; Fig. 2a, b). When multiple phages were added simultaneously to the microcosms, we found that reduction in bacterial growth was

significantly greater than what had been observed for each of the three phages on its own (Fig. 2a, b), clearly indicating that phage richness maximizes the infection of bacterial communities in microcosms.

We expected from theory that phages increase complementarity of bacterial mixtures. Our results showed no significant differences on mean bacterial overyielding in the presence of phages ($F_{4, 2715} = 0.02$; $P > 0.05$; Fig. 2c, d), with average overyielding values for each phage infection being close to 1. These values indicate that bacteria yield in mixtures was not greater than what would have been predicted by the most productive monocultures of either bacteria in the mixture. These results are contrary to recent studies that have shown that multiple predators (i.e. protists) may increase bacterial yields due to an increased complementarity among bacterial species (Saleem et al. 2012). The phages in our experiment were particularly effective in reducing bacterial growth rates, overwhelming any potential positive effects on bacterial mixtures. Our study shows that when considering a wide range of bacterial hosts can result in a wide range of interactions ranging from negative (OV < 1) to positive (OV > 1) interactions (Fig. 2c, d), which might partially explain why there is no overall phages effect on overyielding. A close inspection of Fig 1d shows that a considerable proportion (circa 48%) of the pairs of bacteria showed increased overyielding when phages were added to the microcosms. These results reveal positive effects but these are averaged out when the entire pool of bacterial hosts and all pairwise combination are considered.

We also predicted that bacterial species' complementarity should decrease in presence of phages and therefore reduce the realized niche overlap among pairs of bacteria. We found indeed that the presences of phages significantly decreased niche overlap among bacteria ($F_{4, 2715} = 311.8$; $P < 0.001$; Fig. 2e, f) and that such effect was greatest when all phages are present in the mixture, leading to the greatest reduction of niche overlap.

It has been shown that interactive effects between diversity within each trophic level may have great impacts on microbial ecosystem functioning (Saleem et al. 2013). We found in our experiment that negative effect of phages on bacterial growth rate increases with their diversity. We did not see a change in the yield of bacterial mixtures in comparison to the most productive monoculture (overyielding). The majority of the expected phage effects did occur in bacterial monocultures (Fig. 2), and these effects were not consistently translated into realized effects in bacterial mixtures. We did however found a significant effect of phages on niche overlap, confirming that apparent competition contributes to niche differentiation. The outcome of interactions among pairs of bacterial strains and between bacteria and phages is harder to predict than what was initially expected following the infection trials. A possible explanation is that there were indirect effects of phages that we did not anticipated in mixtures. For example, it has been shown that the presence of bacteriophages may increase bacterial population growth rate without being able to infect bacterial cells (Poisot et al. 2012).

CONCLUSIONS

Our results illustrate how productivity in bacterial microcosms can be affected by the interplay between the outcome of exploitative (shared resources between bacteria) and apparent (shared phages between bacteria) competition. While we found a significant effect of phage on bacterial niche overlap (apparent competition) we did not find an effect of the presence of phage on mean bacterial overyielding in mixtures. These results suggest that understanding the combined effect of resource and predator complementarity on ecosystem functioning is more complex than initially though. This added complexity was not anticipated but revealed diverse microbial ecosystems are likely driven by a combination of combined effects of competition (between bacteria) and predation (between phages and bacteria) and a range of indirect interactions

between bacteria and phages that have not been accounted for in theoretical predictions. Keeping a continuous link between development of ecological theory and experimental testing with microcosm will help disentangling this important feedback loop to advance our understanding of biodiversity and ecosystems at large scales.

STATEMENT OF AUTHORSHIP

MGM, MC and CB conducted fieldwork, bacterial and phage isolation, molecular analysis and experimental trials. MGM, DM, TP and NM conceived the study. MGM and DM conducted data analysis. All the authors contributed for structuring and writing the paper.

ACKNOWLEDGEMENTS

MGM, MC, CB and NM were supported by CNRS and grant ANR-BACH-09-JCJC-0110-01. MGM acknowledges support by a Marie Curie Intra-European Fellowship within the 7th European Community Framework Programme (FORECOMM). DG was supported by the NSERC and the Canada Research Chair program.

REFERENCES

Andrewartha HG, and Birch LC. 1954. *The distribution and abundance of animals*: Univ. Chicago Press.

Cadotte MW, Drake JA, and Fukami T. 2005. Constructing nature: laboratory models as necessary tools for investigating complex ecological communities. *Advances in Ecological Research* 37:333-353.

Chesson P, and Kuang JJ. 2008. The interaction between predation and competition. *Nature* 456:235-238.

Gómez P, and Buckling A. 2011. Bacteria-phage antagonistic coevolution in soil. *Science* 332:106-109.

Goyal SM, and Gerba CP. 1979. Comparative adsorption of human enteroviruses, simian rotavirus, and selected bacteriophages to soils. *Applied and Environmental Microbiology* 38:241-247.

Gravel D, Bell T, Barbera C, Bouvier T, Pommier T, Venail P, and Mouquet N. 2011. Experimental niche evolution alters the strength of the diversity-productivity relationship. *Nature* 469:89-92.

Holt RD. 1977. Predation, apparent competition, and the structure of prey communities. *Theoretical Population Biology* 12:197-229.

Livingston G, Matias M, Calcagno V, Barbera C, Combe M, Leibold MA, and Mouquet N. 2012. Competition-colonization dynamics in experimental bacterial metacommunities. *Nat Commun* 3:1234.

MacArthur R. 1972. Coexistence of species. In: Benke J, ed. *Challenging biological problems*, 253-259.

Matias M, Combe M, Barbera C, and Mouquet N. 2013. Ecological strategies shapes the insurance potential of biodiversity. *Front Microbiol* 3.

Poisot T, Bell T, Martinez E, Gougat-Barbera C, and Hochberg ME. 2012. Terminal investment induced by a bacteriophage in a rhizosphere bacterium. *F1000Research* 1.

Poisot T, Lepennetier G, Martinez E, Ramsayer J, and Hochberg ME. 2011. Resource availability affects the structure of a natural bacteria–bacteriophage community. *Biology Letters* 7:201-204.

Poisot T, Mouquet N, and Gravel D. 2013. Trophic complementarity drives the biodiversity–ecosystem functioning relationship in food webs. *Ecology Letters* 16:853-861.

Saleem M, Fetzer I, Dormann CF, Harms H, and Chatzinotas A. 2012. Predator richness increases the effect of prey diversity on prey yield. *Nat Commun* 3:1305.

Saleem M, Fetzer I, Harms H, and Chatzinotas A. 2013. Diversity of protists and bacteria determines predation performance and stability. *ISME J*.

Thebault E, and Loreau M. 2003. Food-web constraints on biodiversity–ecosystem functioning relationships. *Proceedings of the National Academy of Sciences* 100:14949-14954.

Venail PA, MacLean RC, Bouvier T, Brockhurst MA, Hochberg ME, and Mouquet N. 2008. Diversity and productivity peak at intermediate dispersal rate in evolving metacommunities. *Nature* 452:210-U257.

FIGURES

Figure 1 – Infection matrix of phage isolates (P1, P2 or P3) on a range of 17 bacterial isolates. Each cell indicates the average effect across all replicates for each combination of phage and bacterial monoculture. Cells with darker colours indicate stronger effects of phages on bacterial growth.

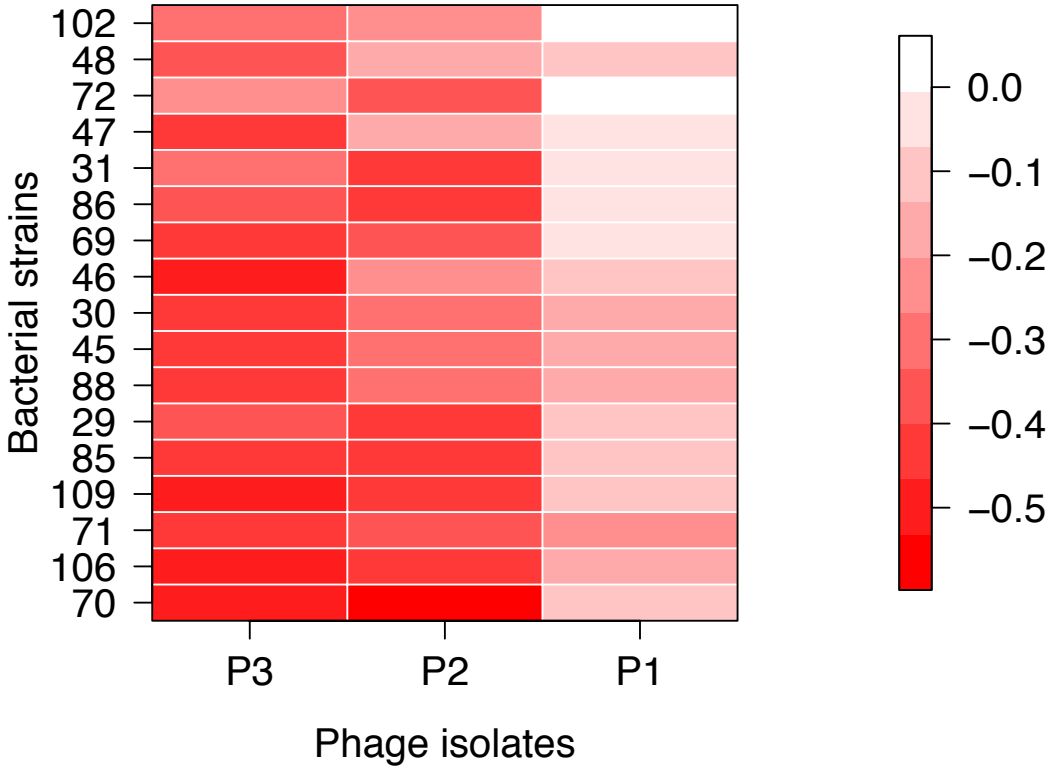

Figure 2 – Impact of phage diversity on bacterial yield (a, b), overyielding (c, d) and overlap (e, f). Phage treatments: controls (M9); monocultures (P1, P2 and P3) or mixtures (PMIX). Note that each boxplot combines the data from all pairs of bacteria for each phage treatment. Letters indicate the results of Tukey multiple comparison of treatment means; treatments with different letters are significant at $P < 0.05$). Plots on the right show comparisons of bacterial mixtures under the presence or absence of phages. The 1:1 line n these plots line indicates values that showed same response under the presence or absence of phages.

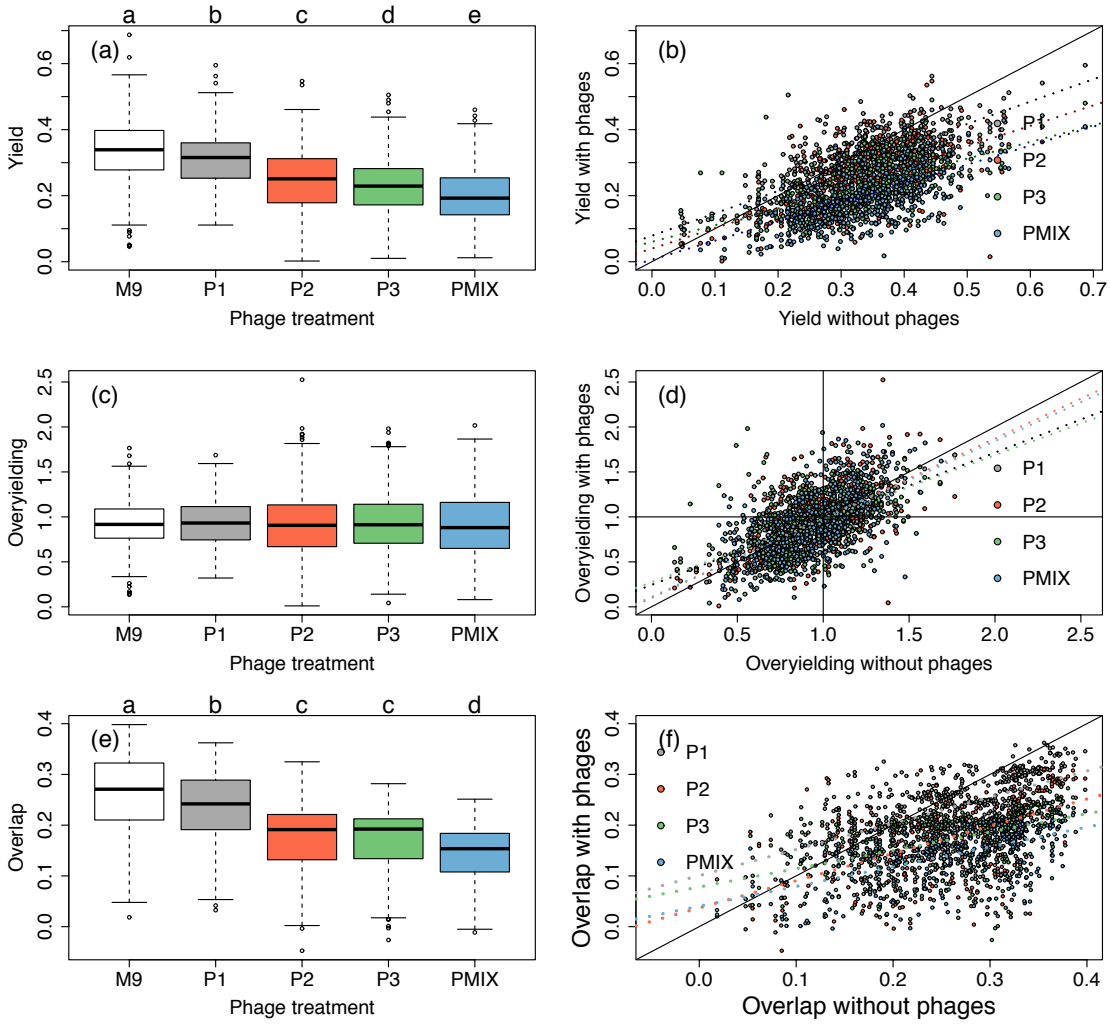

Electronic Supplementary Material: Table S4. NCBI BLAST results for each bacterial strain. Results restricted to sequences with 100% coverage and identity and ranked in descending order of total score.

ID	Description	Max score	Total score	Query cover	E value	Identity	Accession reference
25	Pseudomonas poae RE*1-1-14	2231	11159	100%	0	99%	NC_020209.1
	Pseudomonas syringae pv. phaseolicola 1448A chromosome	2204	11020	100%	0	99%	NC_005773.3
	Pseudomonas syringae pv. syringae B728a chromosome	2204	10993	100%	0	99%	NC_007005.1
	Pseudomonas brassicacearum subsp. brassicacearum NFM421 chromosome	2187	10932	100%	0	99%	NC_015379.1
	Pseudomonas sp. UW4 chromosome	2170	15043	100%	0	99%	NC_019670.1
	Pseudomonas synxantha BG33R chromosome	2159	12912	100%	0	99%	NZ_CM001514.1
	Pseudomonas chlororaphis O6 chromosome	2154	2154	100%	0	99%	NZ_CM001490.1
	Pseudomonas protegens Pf-5 chromosome	2154	10769	100%	0	98%	NC_004129.6
	Pseudomonas syringae pv. tomato str. DC3000 chromosome	2154	10771	100%	0	98%	NC_004578.1
	Pseudomonas fluorescens Pf0-1 chromosome	2109	12654	100%	0	98%	NC_007492.2
30	Pseudomonas putida KT2440 chromosome	2161	15109	100%	0	99%	NC_002947.3
	Pseudomonas monteilii SB3101	2156	12936	100%	0	99%	NC_023076.1
	Pseudomonas entomophila L48 chromosome	2145	15010	100%	0	99%	NC_008027.1
	Pseudomonas sp. UW4 chromosome	2122	14696	100%	0	99%	NC_019670.1
	Pseudomonas mendocina	2087	8340	100%	0	98%	NC_009439.1

	ymp chromosome						
	Pseudomonas syringae pv. phaseolicola 1448A chromosome	2078	10393	100%	0	98%	NC_005773.3
	Pseudomonas fulva 12-X chromosome	2076	8295	100%	0	98%	NC_015556.1
	Pseudomonas syringae pv. syringae B728a chromosome	2073	10343	100%	0	98%	NC_007005.1
	Pseudomonas brassicacearum subsp. brassicacearum NFM421 chromosome	2067	10309	100%	0	98%	NC_015379.1
	Pseudomonas fluorescens Pf0-1 chromosome	2034	12205	100%	0	97%	NC_007492.2
31	Serratia liquefaciens ATCC 27592 plasmid, complete sequence	778	1184	100%	0	100%	NC_021742.1
	Serratia liquefaciens ATCC 27592	778	4621	100%	0	100%	NC_021741.1
	Serratia proteamaculans 568 chromosome	773	5388	100%	0	99%	NC_009832.1
	Pectobacterium sp. SCC3193	745	5084	100%	0	99%	NC_017845.1
	Pectobacterium wasabiae WPP163 chromosome	745	5095	100%	0	99%	NC_013421.1
	Pectobacterium atrosepticum SCRI1043 chromosome	734	5095	100%	0	98%	NC_004547.2
	Serratia plymuthica AS9 chromosome	732	5126	100%	0	98%	NC_015567.1
	Serratia sp. AS12 chromosome	732	5126	100%	0	98%	NC_015566.1
	Rahnella aquatilis HX2 chromosome	723	5045	100%	0	98%	NC_017047.1
	Rahnella sp. Y9602 chromosome	723	5062	100%	0	98%	NC_015061.1
45	Pseudomonas putida KT2440 chromosome	2241	15665	100%	0	99%	NC_002947.3
	Pseudomonas monteilii SB3101	2224	13346	100%	0	99%	NC_023076.1
	Pseudomonas entomophila L48 chromosome	2224	15565	100%	0	99%	NC_008027.1

	Pseudomonas fulva 12-X chromosome	2150	8591	100%	0	98%	NC_015556.1
	Pseudomonas sp. UW4 chromosome	2135	14786	100%	0	98%	NC_019670.1
	Pseudomonas syringae pv. syringae B728a chromosome	2113	10546	100%	0	98%	NC_007005.1
	Pseudomonas stutzeri A1501 chromosome	2108	8382	100%	0	98%	NC_009434.1
	Pseudomonas syringae pv. phaseolicola 1448A chromosome	2108	10540	100%	0	98%	NC_005773.3
	Pseudomonas mendocina ymp chromosome	2100	8391	100%	0	98%	NC_009439.1
	Pseudomonas brassicacearum subsp. brassicacearum NFM421 chromosome	2091	10429	100%	0	97%	NC_015379.1
46	Pseudomonas putida KT2440 chromosome	2196	15355	100%	0	99%	NC_002947.3
	Pseudomonas monteilii SB3101	2180	13081	100%	0	99%	NC_023076.1
	Pseudomonas entomophila L48 chromosome	2180	15255	100%	0	99%	NC_008027.1
	Pseudomonas fulva 12-X chromosome	2106	8414	100%	0	98%	NC_015556.1
	Pseudomonas sp. UW4 chromosome	2091	14476	100%	0	98%	NC_019670.1
	Pseudomonas syringae pv. syringae B728a chromosome	2069	10324	100%	0	98%	NC_007005.1
	Pseudomonas stutzeri A1501 chromosome	2063	8205	100%	0	98%	NC_009434.1
	Pseudomonas syringae pv. phaseolicola 1448A chromosome	2063	10319	100%	0	98%	NC_005773.3
	Pseudomonas mendocina ymp chromosome	2056	8214	100%	0	98%	NC_009439.1
	Pseudomonas brassicacearum subsp. brassicacearum NFM421 chromosome	2047	10208	100%	0	97%	NC_015379.1
47	Pseudomonas putida KT2440	2161	15109	100%	0	99%	NC_002947.3

	chromosome						
	Pseudomonas monteilii SB3101	2145	12870	100%	0	99%	NC_023076.1
	Pseudomonas entomophila L48 chromosome	2145	15010	100%	0	99%	NC_008027.1
	Pseudomonas fulva 12-X chromosome	2076	8295	100%	0	98%	NC_015556.1
	Pseudomonas sp. UW4 chromosome	2056	14230	100%	0	98%	NC_019670.1
	Pseudomonas syringae pv. syringae B728a chromosome	2043	10195	99%	0	98%	NC_007005.1
	Pseudomonas syringae pv. phaseolicola 1448A chromosome	2037	10189	99%	0	98%	NC_005773.3
	Pseudomonas stutzeri A1501 chromosome	2034	8070	100%	0	98%	NC_009434.1
	Pseudomonas mendocina ymp chromosome	2026	8102	100%	0	98%	NC_009439.1
	Pseudomonas brassicacearum subsp. brassicacearum NFM421 chromosome	2021	10079	99%	0	98%	NC_015379.1
48	Pseudomonas putida KT2440 chromosome	2244	15691	100%	0	99%	NC_002947.3
	Pseudomonas monteilii SB3101	2228	13369	100%	0	99%	NC_023076.1
	Pseudomonas entomophila L48 chromosome	2228	15591	100%	0	99%	NC_008027.1
	Pseudomonas fulva 12-X chromosome	2154	8606	100%	0	98%	NC_015556.1
	Pseudomonas sp. UW4 chromosome	2139	14812	100%	0	98%	NC_019670.1
	Pseudomonas syringae pv. syringae B728a chromosome	2117	10564	100%	0	98%	NC_007005.1
	Pseudomonas stutzeri A1501 chromosome	2111	8397	100%	0	98%	NC_009434.1
	Pseudomonas syringae pv. phaseolicola 1448A chromosome	2111	10559	100%	0	98%	NC_005773.3
	Pseudomonas mendocina	2104	8406	100%	0	98%	NC_009439.1

	ymp chromosome						
	Pseudomonas brassicacearum subsp. brassicacearum NFM421 chromosome	2095	10448	100%	0	97%	NC_015379.1
69	Enterobacter aerogenes KCTC 2190 chromosome	1679	13421	100%	0	99%	NC_015663.1
	Enterobacter sp. 638	1674	11697	100%	0	99%	NC_009436.1
	Klebsiella oxytoca KCTC 1686 chromosome	1668	13188	100%	0	99%	NC_016612.1
	Raoultella ornithinolytica B6	1663	13199	100%	0	99%	NC_021066.1
	Enterobacter asburiae LF7a chromosome	1663	11540	100%	0	99%	NC_015968.1
	Pantoea vagans C9-1 chromosome	1624	11187	100%	0	98%	NC_014562.1
	Klebsiella pneumoniae subsp. pneumoniae MGH 78578 chromosome	1620	12881	99%	0	98%	NC_009648.1
	Klebsiella variicola At-22 chromosome	1615	12802	99%	0	98%	NC_013850.1
	Pantoea ananatis LMG 20103 chromosome	1602	11119	100%	0	98%	NC_013956.2
	Klebsiella pneumoniae subsp. pneumoniae HS11286 chromosome	1591	12667	99%	0	98%	NC_016845.1
70	Enterobacter sp. 638	2134	14899	100%	0	99%	NC_009436.1
	Klebsiella oxytoca KCTC 1686 chromosome	2100	16628	100%	0	99%	NC_016612.1
	Enterobacter asburiae LF7a chromosome	2084	14564	100%	0	98%	NC_015968.1
	Raoultella ornithinolytica B6	2073	16534	100%	0	98%	NC_021066.1
	Enterobacter aerogenes KCTC 2190 chromosome	2073	16578	100%	0	98%	NC_015663.1
	Enterobacter cloacae SCF1 chromosome	2073	14448	100%	0	98%	NC_014618.1
	Enterobacter cloacae subsp. cloacae ATCC 13047 chromosome	2045	16276	100%	0	98%	NC_014121.1

	Klebsiella pneumoniae subsp. pneumoniae MGH 78578 chromosome	2039	16191	100%	0	98%	NC_009648.1
	Klebsiella variicola At-22 chromosome	2034	16156	100%	0	98%	NC_013850.1
	Salmonella enterica subsp. enterica serovar Typhimurium str. LT2 chromosome	2023	14029	100%	0	98%	NC_003197.1
71	Klebsiella oxytoca KCTC 1686 chromosome	1676	13136	100%	0	99%	NC_016612.1
	Raoultella ornithinolytica B6	1664	13170	100%	0	99%	NC_021066.1
	Enterobacter aerogenes KCTC 2190 chromosome	1664	13194	100%	0	99%	NC_015663.1
	Enterobacter asburiae LF7a chromosome	1631	11320	100%	0	98%	NC_015968.1
	Enterobacter sp. 638	1631	11399	100%	0	98%	NC_009436.1
	Pantoea vagans C9-1 chromosome	1592	10945	100%	0	98%	NC_014562.1
	Klebsiella pneumoniae subsp. pneumoniae MGH 78578 chromosome	1587	12544	100%	0	97%	NC_009648.1
	Pantoea ananatis LMG 20103 chromosome	1576	10978	100%	0	97%	NC_013956.2
	Klebsiella variicola At-22 chromosome	1576	12514	100%	0	97%	NC_013850.1
	Klebsiella pneumoniae subsp. pneumoniae HS11286 chromosome	1563	12435	100%	0	97%	NC_016845.1
72	Klebsiella oxytoca KCTC 1686 chromosome	1594	12508	100%	0	99%	NC_016612.1
	Raoultella ornithinolytica B6	1578	12501	100%	0	99%	NC_021066.1
	Enterobacter aerogenes KCTC 2190 chromosome	1578	12503	100%	0	99%	NC_015663.1
	Enterobacter sp. 638	1554	10856	99%	0	99%	NC_009436.1
	Enterobacter asburiae LF7a chromosome	1544	10735	100%	0	99%	NC_015968.1
	Klebsiella pneumoniae subsp. pneumoniae MGH 78578 chromosome	1517	11982	100%	0	98%	NC_009648.1

	Pantoea vagans C9-1 chromosome	1511	10397	100%	0	98%	NC_014562.1
	Klebsiella variicola At-22 chromosome	1506	11956	100%	0	98%	NC_013850.1
	Pantoea ananatis LMG 20103 chromosome	1495	10410	100%	0	97%	NC_013956.2
	Klebsiella pneumoniae subsp. pneumoniae HS11286 chromosome	1493	11873	100%	0	97%	NC_016845.1
85	Aeromonas hydrophila subsp. hydrophila ATCC 7966 chromosome	2211	22104	100%	0	99%	NC_008570.1
	Aeromonas salmonicida subsp. salmonicida A449	2145	19294	100%	0	99%	NC_009348.1
	Aeromonas veronii B565 chromosome	2117	21112	100%	0	98%	NC_015424.1
	Tolumonas auensis DSM 9187 chromosome	1773	14113	100%	0	93%	NC_012691.1
	Cronobacter turicensis z3032 chromosome	1668	11674	100%	0	92%	NC_013282.2
	Shewanella sp. ANA-3 chromosome 1, complete sequence	1663	14868	100%	0	92%	NC_008577.1
	Shewanella baltica OS223 chromosome	1657	16509	100%	0	92%	NC_011663.1
	Shewanella pealeana ATCC 700345 chromosome	1657	18227	100%	0	92%	NC_009901.1
	Shewanella baltica OS185 chromosome	1657	16531	100%	0	92%	NC_009665.1
	Shewanella baltica OS155 chromosome	1657	16536	100%	0	92%	NC_009052.1
86	Enterobacter sp. 638	2287	15844	99%	0	99%	NC_009436.1
	Klebsiella oxytoca KCTC 1686 chromosome	2259	17843	99%	0	99%	NC_016612.1
	Enterobacter cloacae SCF1 chromosome	2237	15576	99%	0	99%	NC_014618.1
	Raoultella ornithinolytica B6	2226	17760	99%	0	98%	NC_021066.1
	Enterobacter aerogenes KCTC 2190 chromosome	2226	17805	99%	0	98%	NC_015663.1

	Enterobacter asburiae LF7a chromosome	2220	15521	99%	0	98%	NC_015968.1
	Klebsiella pneumoniae subsp. pneumoniae MGH 78578 chromosome	2193	17417	99%	0	98%	NC_009648.1
	Enterobacter cloacae subsp. cloacae ATCC 13047 chromosome	2187	17409	99%	0	98%	NC_014121.1
	Klebsiella variicola At-22 chromosome	2187	17382	99%	0	98%	NC_013850.1
	Klebsiella pneumoniae subsp. pneumoniae HS11286 chromosome	2163	17269	99%	0	97%	NC_016845.1
102	Klebsiella oxytoca KCTC 1686 chromosome	1936	15286	100%	0	99%	NC_016612.1
	Enterobacter aerogenes KCTC 2190 chromosome	1925	15286	100%	0	99%	NC_015663.1
	Enterobacter sp. 638	1919	13394	100%	0	98%	NC_009436.1
	Enterobacter cloacae subsp. cloacae ATCC 13047 chromosome	1905	15169	99%	0	98%	NC_014121.1
	Enterobacter asburiae LF7a chromosome	1897	13204	100%	0	98%	NC_015968.1
	Citrobacter koseri ATCC BAA-895 chromosome	1893	12914	99%	0	98%	NC_009792.1
	Salmonella enterica subsp. enterica serovar Typhimurium str. LT2 chromosome	1893	13152	99%	0	98%	NC_003197.1
	Raoultella ornithinolytica B6	1881	15003	100%	0	98%	NC_021066.1
	Klebsiella pneumoniae subsp. pneumoniae MGH 78578 chromosome	1877	14935	99%	0	98%	NC_009648.1
	Salmonella enterica subsp. enterica serovar Typhi str. CT18	1877	13135	99%	0	98%	NC_003198.1
106	Aeromonas salmonicida subsp. salmonicida A449	2237	20081	100%	0	99%	NC_009348.1
	Aeromonas hydrophila subsp. hydrophila ATCC 7966 chromosome	2176	21753	100%	0	99%	NC_008570.1

	Aeromonas veronii B565 chromosome	2154	21448	100%	0	99%	NC_015424.1
	Tolumonas auensis DSM 9187 chromosome	1799	14237	100%	0	93%	NC_012691.1
	Shewanella denitrificans OS217	1716	13700	100%	0	92%	NC_007954.1
	Shewanella baltica OS223 chromosome	1709	17015	99%	0	92%	NC_011663.1
	Shewanella baltica OS185 chromosome	1709	16970	99%	0	92%	NC_009665.1
	Shewanella sp. ANA-3 chromosome 1, complete sequence	1709	15289	99%	0	92%	NC_008577.1
	Shewanella sp. MR-7 chromosome	1709	15150	99%	0	92%	NC_008322.1
	Shewanella halifaxensis HAW-EB4 chromosome	1705	17055	100%	0	92%	NC_010334.1
109	Aeromonas salmonicida subsp. salmonicida A449	2242	20131	100%	0	99%	NC_009348.1
	Aeromonas hydrophila subsp. hydrophila ATCC 7966 chromosome	2182	21809	100%	0	99%	NC_008570.1
	Aeromonas veronii B565 chromosome	2159	21504	100%	0	99%	NC_015424.1
	Tolumonas auensis DSM 9187 chromosome	1805	14281	100%	0	93%	NC_012691.1
	Shewanella denitrificans OS217	1722	13744	100%	0	92%	NC_007954.1
	Shewanella baltica OS223 chromosome	1714	17070	99%	0	92%	NC_011663.1
	Shewanella baltica OS185 chromosome	1714	17026	99%	0	92%	NC_009665.1
	Shewanella sp. ANA-3 chromosome 1, complete sequence	1714	15339	99%	0	92%	NC_008577.1
	Shewanella sp. MR-7 chromosome	1714	15200	99%	0	92%	NC_008322.1
	Shewanella halifaxensis HAW-EB4 chromosome	1711	17111	100%	0	92%	NC_010334.1

PeerJ PrePrints | https://dx.doi.org/10.7287/peerj.preprints.1190v1 | CC-BY 4.0 Open Access | rec: 19 May 2015, publ: 19 May 2015

Electronic Supplementary Material S2
Bacteriophage richness reduces bacterial niche overlap in experimental microcosms

May 19, 2015

Derivation of a measure of niche overlap for a two-species system

This appendix describes the derivation of a measure of niche overlap for a two-species system based on their population sizes in monocultures. We consider a simple model of lotka-volterrra competition:

$$\frac{dN_1}{dt} = r_1 N_1 (1 - \frac{N_1 - a_{12} N_2}{K_1}) \quad (1)$$

$$\frac{dN_2}{dt} = r_2 N_2 (1 - \frac{N_2 - a_{21} N_1}{K_2}) \quad (2)$$

where a_{12} and a_{21} are the interspecific interaction coefficients of species 1 and species 2 and N_1 and N_2 are the population sizes of each species. Assuming that we know the equilibrium density of species 1 (K_1) and species 2 (K_1) in isolation, and of their total density in mixture (K_{12}), we find the following system of equations describing the equilibrium densities in mixtures (named N_1^* and N_2^*):

$$N_1^* = (1 - a_{12} N_2) K_1 \quad (3)$$

$$N_2^* = (1 - a_{21} N_1) K_2 \quad (4)$$

$$K_{12} = N_1^* + N_2^* \quad (5)$$

To simplify this system we assume that niche overlap is symetric between the species. Critical conditions for coexistence can be determined by the ratio of interaction coefficients or carrying capacities (Chesson and Kuang, 2008):

$$a_{ij}/a_{jj} = \rho K_j / K_i \quad (6)$$

PeerJ PrePrints | https://dx.doi.org/10.7287/peerj.preprints.1100v1 | CC-BY 4.0 Open Access | rec: 19 May 2015, publ: 19 May 2015

where ρ is the coefficient of niche overlap. Coexistence requires Eq. 6 to be smaller than 1. Rearranging the equation to isolate the coefficient of interspecific competition we get:

$$a_{ij} = \rho a_{jj} K_j / K_i \tag{7}$$

Since $a_{jj} = K_j^{-1}$, the system can be simplified to:

$$a_{ij} = \rho / K_i \tag{8}$$

Introducing Eq. 8 into Eqs 3-4 we obtain:

$$N_1^* = K_1 - \rho N_2^* / K_1 \tag{9}$$

$$N_2^* = K_2 - \rho N_1^* / K_2 \tag{10}$$

By substituing Eq. 5 into Eqs. 9-10, we obtain two solutions for the measure of niche overalp that are strickly dependent on the equilibrium densities in isolation and in mixture:

$$\rho_1 = \frac{K_1^2 + K_2^2 + \sqrt{K_1^4 + K_2^4 + K_1 K_2 (2K_1 K_2 - 4K_{12}(K_1 + K_2 - K_{12}))}}{2K_{12}} \tag{11}$$

$$\rho_2 = \frac{K_1^2 + K_2^2 - \sqrt{K_1^4 + K_2^4 + K_1 K_2 (2K_1 K_2 - 4K_{12}(K_1 + K_2 - K_{12}))}}{2K_{12}} \tag{12}$$

.

PeerJ PrePrints | https://dx.doi.org/10.7287/peerj.preprints.1100v1 | CC-BY 4.0 Open Access | rec: 19 May 2015, publ: 19 May 2015